

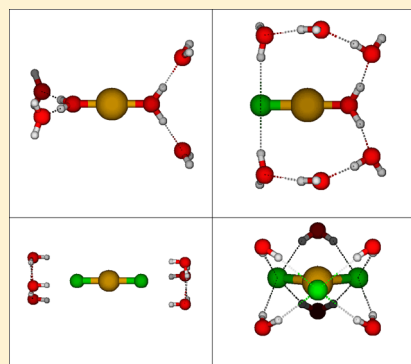
Raman and ab Initio Investigation of Aqueous Cu(I) Chloride Complexes from 25 to 80 °C

Lucas M. S. G. A. Applegarth,[†] Christopher R. Corbeil,[‡] Darren J. W. Mercer,[‡] Cory C. Pye,^{‡,§} and Peter R. Tremaine^{*,†,||}

[†]Department of Chemistry, University of Guelph, Guelph, Ontario, Canada N1G 2W1

[‡]Department of Chemistry, Saint Mary's University, Halifax, Nova Scotia, Canada B3H 3C3

ABSTRACT: Temperature-dependent Raman studies of aqueous copper(I) chloride complexes have been carried out up to 80 °C, along with supporting ab initio calculations for the species $[\text{CuCl}_n(\text{H}_2\text{O})_m]^{1-n}$, $n = 0-4$ and hydration numbers $m = 0-6$. Normalized reduced isotropic Raman spectra were obtained from perpendicular and parallel polarization measurements, with perchlorate anion, ClO_4^- , as an internal standard. Although the Raman spectra were not intense, spectra could be corrected by solvent baseline subtraction, to yield quantitative reduced molar scattering coefficients for the symmetric vibrational bands at 297 ± 3 and $247 \pm 3 \text{ cm}^{-1}$. The intensity variations of these bands with concentration and temperature provided strong evidence that these arise from the species $[\text{CuCl}_2]^-$ and $[\text{CuCl}_3]^{2-}$, respectively. The results from ab initio calculations using density functional theory predict similar relative peak positions and intensities for the totally symmetric Cu–Cl stretching bands of the species $[\text{CuCl}_2(\text{H}_2\text{O})_6]^-$ and $[\text{CuCl}_3(\text{H}_2\text{O})_6]^{2-}$, in which the water is coordinated to the chloride ions. A less intense Raman band at $350 \pm 10 \text{ cm}^{-1}$ is attributed to the symmetric Cu–Cl stretching mode of hydrated species $[\text{CuCl}(\text{H}_2\text{O})]_0$ with six waters of hydration. Temperature- and concentration-independent quantitative Raman molar scattering coefficients (S) are reported for the $[\text{CuCl}_2]^-$ and $[\text{CuCl}_3]^{2-}$ species.



1. INTRODUCTION

The thermodynamic properties of the aqueous complexes of copper(I) and copper(II) with common ligands under hydrothermal conditions are needed to model the chemistry of advanced designs for the steam generators used in thermal and nuclear electric power stations,¹ thermochemical hydrogen production technologies,² and the geochemistry of metal ore deposits.^{3,4} The effects of temperature on the formation constants of copper with the chloride ion have been under investigation for many years. (See, for example: Crerar and Barnes,⁵ Ahrlund and Rawsthorne,⁶ Seward and Mountain,^{7,8} Sharma and Millero,⁹ Fritz,^{10,11} Brugger et al.,^{12,13} and Trevani et al.¹⁴) Although the thermodynamic stabilities of the copper(I) and copper(II) chloro complexes are now quite well established over a wide temperature range, the structure of some of these species is a subject of active investigation.

The thermodynamic properties of the copper(II) chloro-complexes, $[\text{CuCl}_n(\text{H}_2\text{O})_m]^{2-n}$ have been studied by UV–visible spectroscopy,^{12,14} electrochemical methods,¹⁵ X-ray absorption spectroscopy (XAS),^{16–18} and computational techniques using both density functional theory (DFT)^{19,20} and molecular dynamics (MD).^{17,21,22} The number of species is still under discussion as various authors show evidence for the formation of complexes containing up to four or five chloride ions.

Studies of the chloro-complexes of copper(I) chloride are more challenging, because the solutions are sensitive to oxygen and can disproportionate to form aqueous copper(II) species

and copper metal.^{23,24} The experimental techniques used to determine the thermodynamic properties and speciation of copper(I) chloro-complexes, $[\text{CuCl}_n(\text{H}_2\text{O})_m]^{1-n}$, under hydrothermal conditions include mass spectrometry,³ solubility,^{3,25–27} UV–visible spectroscopy,²⁸ XAS,^{13,17,29–34} and computational techniques.^{35,36} These show that the stable chloride complexes of copper(I) are $[\text{CuCl}]^0$, $[\text{CuCl}_2]^-$, and $[\text{CuCl}_3]^{2-}$. A few experiments indicated the existence of a more highly coordinated species, which was speculated to be $[\text{CuCl}_4]^{3-}$.^{25,37,38} Further analysis of this species showed that it would be unstable in aqueous media and it has since been discredited.¹³ Ahrlund et al.,⁶ Fritz,¹⁰ and Brugger et al.³³ have reported polynuclear Cu(I) species, such as $[\text{Cu}_2\text{Cl}_4]^{2-}$. A polynuclear species that includes two oxidation states of copper, $[\text{Cu}_2\text{Cl}_3]^0$, has been reported by McConnell and Davidson.³⁹ More recent experimental and computational studies show no evidence for dimers or trimers as stable species.

Ab initio calculations have proven to be useful in identifying the structures of stable metal aqua-complexes, which can then be compared with the vibrational spectra obtained from quantitative Raman spectroscopy (see, for example, Rudolph et al.^{40–43}). Recent studies by one of the authors have applied this approach to the chloro-complexes of lithium,⁴⁴ zinc(II),⁴⁵ and scandium(III).⁴⁶ Good agreement was found between

Received: July 3, 2013

Revised: November 14, 2013

Published: November 20, 2013

experiment and theory, provided the systematic errors due to the level of theory and hydration effects were taken into account. A few very recent studies have attempted to use ab initio methods to predict the stability and structures of the aqueous chloro-complexes of copper(II). For example, Yi et al.¹⁹ used density functional theory to calculate the structures of the copper(II) species $[\text{CuCl}_3]^-$ (aq) and $[\text{CuCl}_4]^{2-}$ (aq). Li et al.¹⁸ reported DFT calculations for copper(II) chloro-complexes in aqueous ionic liquid mixtures, and compared the results with XAFS and UV–visible spectroscopic results. A recent paper by Brugger et al.³⁶ has reported ab initio molecular dynamics calculations of copper(I) complexation in chloride and bisulfide hydrothermal fluids.

The present study utilized both Raman spectroscopy and ab initio methods to determine the structure and vibrational spectra of the copper(I) chloro-complexes in aqueous media at temperatures up to 80 °C. Raman spectra were recorded in solutions of 6 mol·kg⁻¹ HCl(aq) as a function of copper(I) and chloride concentrations. The variations in the intensity of the vibrational bands with concentration and temperature were compared to speciation calculations based on the thermodynamic constants reported by Liu et al.²⁸ to assign the bands to $[\text{CuCl}_2]^-$ and $[\text{CuCl}_3]^{2-}$. These assignments were then compared to the vibrational spectra predicted from ab initio calculations for copper(I) chloro complexes of the form $[\text{CuCl}_n(\text{H}_2\text{O})_m]^{1-n}$ to identify structure. Attempts to obtain data at temperatures greater than 100 °C were limited by disproportionation reactions.

2. EXPERIMENTAL METHODS

2.1. Chemicals and Solution Preparation. Copper wire (1 mm diameter, >99.9%) and copper(I) chloride (Reagent-Plus, purified >99.9%) were purchased from Sigma-Aldrich. Concentrated hydrochloric acid was purchased from Acros with no further purification. The water used was Milli-Q nanopure water with an electrical resistivity of 18.2 MΩ cm. All preparations and measurements were carried out in an inert atmosphere to avoid the oxidation of copper(I) to copper(II).

The 6 mol·kg⁻¹ HCl solutions were prepared to the approximate concentration and then standardized by diluting a weighed aliquot and titrating it with a standard solution of 0.1 mol kg⁻¹ NaOH. Copper wire was placed in the acidic solutions, which were further purged for 5–10 min using argon. For quantitative measurements, the perchlorate anion is commonly used as an internal reference as it is a strong Raman scattering molecule and a noncomplexing anion. Anhydrous sodium perchlorate (Alpha Aesar, ACS Reagent grade, dried to constant mass at 110 °C) was added by mass to provide a final concentration 0.1 mol·kg⁻¹ of ClO_4^- . The solutions were left sealed under an inert argon atmosphere for 2–3 days to allow for the reaction with copper wire to remove any remaining oxygen from the solutions. The copper(I) chloride was then added to the solution by mass in an inert atmosphere to the desired concentration and then sealed and left to stabilize until the solution turned transparent and colorless (approximately 1 week). All dilutions and titrations were carried out by mass, in triplicate, under an inert atmosphere using Milli-Q purified water degassed by argon.

2.2. Raman Instrumentation and Methods. The Raman spectra were recorded with a custom-made Horiba Jobin Yvon HR800 LabRAM spectrometer constructed with both a microprobe and a large macrochamber. The instrument is equipped with an 800 mm focal length spectrograph; a 532 nm,

250 mW, Torus-200 diode-pumped solid-state (DPSS) laser; an edge filter with a Stokes edge of less than 120 cm⁻¹; a 1024 × 256 pixel CCD detector that is Peltier-cooled to approximately –60 °C; an 1800 line/mm holographic grating; a polarizer; and a scrambler. The measurements were carried out in the macrochamber, using a sample cell holder equipped with a calibrated Peltier heater/cooler element. Cell temperatures were measured by an RTD located inside the thermostated compartment near the sample tubes and input to a computer using an MCC USB-Temp high resolution analog-to-digital converter (ADC). LabView VM software used this information to control the voltage level and polarity applied to the Peltier device, which in turn controlled the cell temperature to provide a thermal stability of ±0.10 °C.

Solutions for study by Raman spectroscopy were sealed in cells constructed from commercially available Pyrex tubing (ca. 5.0 mm outer diameter (o.d.) and 3.0 mm inner diameter (i.d.) and ca. 130 mm in height). The Pyrex cells were loaded with the solutions and two pieces of solid copper wire (ca. 10 mm) under an inert atmosphere to a solution level of ca. 50 mm in height, capped to stop any intake of oxygen when removed from the inert atmosphere, and sealed under a torch quickly. Filled cells were no less than 100 mm in length. The sealed cells were pressure tested in an oven at a temperature 25 °C above the experimental temperature to ensure mechanical integrity. No thermal decomposition was observed up to 80 °C. At temperatures of 100 °C and above, the solution turned opaque and brown in color, and decomposition products could be observed from changes in the Raman spectra.

Stokes Raman spectra of solutions in the Pyrex tubes described above were collected at 90° scattering angle geometry, with slit widths of 1000 μm, at both parallel and perpendicular polarizations relative to the exciting line. For each polarization orientation, nine spectra were taken and averaged to minimize the background noise. Spectra were also obtained for the same acid solutions, without the copper(I) chloride and sodium perchlorate, in identical Pyrex tubes, before and after the series of runs for use in baseline corrections.

2.3. Chemical Equilibrium Model. The solution compositions selected for study, and the relative abundances of the species $[\text{CuCl}_n]^{1-n}$ (aq) at 25 and 80 °C used to interpret the Raman results, were calculated from the cumulative formation constants reported by Liu et al.²⁸ These are listed in Table 1, as a function of temperature. The calculations were done with the commercial chemical modeling software MULTEQ (Electric Power Res. Inst., 2006), using an activity coefficient model based on aqueous NaCl, according to the expression $\log \gamma_i = z_i^2 \log \gamma_{\text{NaCl}}$, as described by Lindsay.⁴⁷

2.4. Ab Initio Computational Methods. Preliminary calculations were performed using Gaussian 98.⁴⁸ The MP2 calculations utilize the frozen core approximation. The geometries were optimized using a stepping stone approach, in which the geometries at the levels HF/STO-3G, HF/3-21G, HF/6-31G*, HF/6-31+G*, MP2/6-31G*, and MP2/6-31+G* were sequentially optimized, with the geometry and molecular orbital reused for the subsequent level. When this approach failed (as one or more ligands dissociated or underwent pseudorotation), the problematic level was skipped. Default optimization specifications were normally used. After each level, where possible, a frequency calculation was performed at the same level and the resulting Hessian was used in the following optimization. Z-matrix coordinates constrained to the appro-

Table 1. Values of Cumulative Formation Constants for Copper(I) Chloride Complexes, $\log K_n$, Refitted from Liu et al.,²⁸ Used in Chemical Equilibrium Calculations, $\text{Cu}^+ + n\text{Cl}^- \rightleftharpoons [\text{CuCl}_n]^{(1-n)-}$

temperature (°C)	$[\text{CuCl}]^0$ $\log K_1$	$[\text{CuCl}_2]^-$ $\log K_2$	$[\text{CuCl}_3]^{2-}$ $\log K_3$	$[\text{CuCl}_4]^{3-}$ $\log K_4$
25	4.18	5.47	4.76	2.80
80	3.86	5.18	4.10	1.64
100	3.83	5.15	3.98	1.48
150	3.78	5.11	3.75	1.21
200	3.79	5.14	3.64	1.16
250	3.94	5.30	3.74	1.56
300	4.33	5.67	4.14	2.65
350	4.99	6.32	4.92	4.62

$$\log K_1 = \log \left[\frac{a([\text{CuCl}]^0)}{a(\text{Cu}^+) a(\text{Cl}^-)} \right], \quad \sigma = 0.0389$$

$$\log K_2 = \log \left[\frac{a([\text{CuCl}_2]^-)}{a(\text{Cu}^+) a(\text{Cl}^-)^2} \right], \quad \sigma = 0.0390$$

$$\log K_3 = \log \left[\frac{a([\text{CuCl}_3]^{2-})}{a(\text{Cu}^+) a(\text{Cl}^-)^3} \right], \quad \sigma = 0.0526$$

$$\log K_4 = \log \left[\frac{a([\text{CuCl}_4]^{3-})}{a(\text{Cu}^+) a(\text{Cl}^-)^4} \right], \quad \sigma = 0.1231$$

where σ = standard deviation of fitted function for $\log K_n$ vs T and $a_i = m_i \gamma_i$ is the activity of species i .

appropriate symmetry were used as required to speed up the optimizations. Because frequency calculations are done at each level, any problems with the Z-matrix coordinates would manifest themselves by giving imaginary frequencies corresponding to modes orthogonal to the spanned Z-matrix space. The Hessian was evaluated at the first geometry (opt = CalcFC) for the first level in a series to aid geometry convergence. For structures that proved not to be local minima at the HF/6-31G* level, the subsequent calculations were not performed.

The calculated structures proved to be very sensitive to the choice of theoretical level, with large changes in optimum geometry sometimes between two sequential calculations. In addition, calculations using the low-level basis sets often converged to incorrect copper configurations (s^2d^8 or s^1d^9 instead of d^{10}) that were propagated throughout the calculations, as demonstrated by wave function stability calculations. It was decided to repeat all calculations starting with the highest possible symmetry and systematically desymmetrizing at all appropriate levels, skipping the STO-3G and 3-21G levels. In addition, the use of the 6-311+G* basis set and the B3LYP functional was explored. Great pains were taken to ensure that all relevant minima were found. Only a synopsis of the results will be presented here. The complete study of the $[\text{CuCl}_n(\text{H}_2\text{O})_m]^{1-n}$ system ($n = 0-4$; $m = 0-7$) system will be reported elsewhere.

3. RESULTS

3.1. Raman Spectra. Copper(I) chloride was found to have a very small scattering efficiency and, as such, yielded very low intensity spectra. Quantitative baseline-corrected spectra from

the parallel and perpendicular polarizations, $I_{\parallel}(\omega)$ and $I_{\perp}(\omega)$, were successfully measured up to 80 °C. As an example, Figure 1 shows the polarized spectra, $I_{\parallel}(\omega)$ and $I_{\perp}(\omega)$, for the most

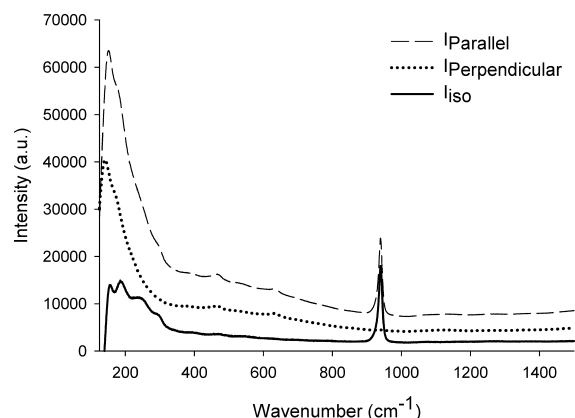


Figure 1. Isotropic, parallel, and perpendicular spectra for 1.5 mol·kg⁻¹ CuCl in 6 mol·kg⁻¹ HCl, with 0.1 mol·kg⁻¹ ClO₄⁻.

concentrated copper(I) chloride solution at 25 °C, and the corresponding isotropic spectrum $I_{\text{iso}}(\omega)$. Following the approach used by Brooker et al.⁴⁹ and others,^{43,50} these were combined to yield the isotropic spectrum:

$$I_{\text{iso}}(\omega) = I_{\parallel}(\omega) - \frac{4}{3}I_{\perp}(\omega) \quad (1)$$

The contribution of the solvent was removed by subtracting the isotropic spectrum for the acid solution. The reproducibility of spectra of the same acid solution in different tubes on the same day was about $\pm 10\%$, and no scaling factor was used for the solvent baseline correction. A further baseline correction was applied to each spectrum by subtracting a quadratic function that passed through the nodes at 175, 460, and 600 cm⁻¹. These frequencies correspond to minima in the solvent-corrected, reduced isotropic spectra for the copper chloride solutions at both 25 and 80 °C.

The isotropic spectrum $I_{\text{iso}}(\omega)$ contains contributions from Rayleigh-wing scattering (Poley absorption) and the thermal excitation of low frequency modes. These are described by the expression,

$$I_{\text{iso}}(\omega) = C_{\text{Instr}}(\omega_0 - \omega)^4 \omega^{-1} B^{-1} S_j \quad (2)$$

$$B = [1 - \exp^{-(h\omega/kT)}] \quad (3)$$

where C_{Instr} is a constant that depends on the instrument response, slit-width, solid collection angle, and absorption due to color; ω_0 is the absolute frequency of the incident laser, in wavenumber units; ω is the frequency difference of the scattered radiation (i.e., the Raman shift); B is the Boltzmann distribution for the thermal population of low frequency excited states; and S_j is the intrinsic molar scattering activity for a Raman scattering process associated with species j . To remove these effects, our data treatment is based on the reduced isotropic form of the spectrum, $R_{\text{iso}}(\omega)$,

$$R_{\text{iso}}(\omega) = I_{\text{iso}}(\omega)(\omega_0 - \omega)^{-4} \omega B \quad (4)$$

The reduced isotropic Raman spectra $R_{\text{iso}}(\omega)$ were calculated from $I_{\text{iso}}(\omega)$ using eqs 3 and 4, by a software program written in Wolfram Mathematica version 5.0.

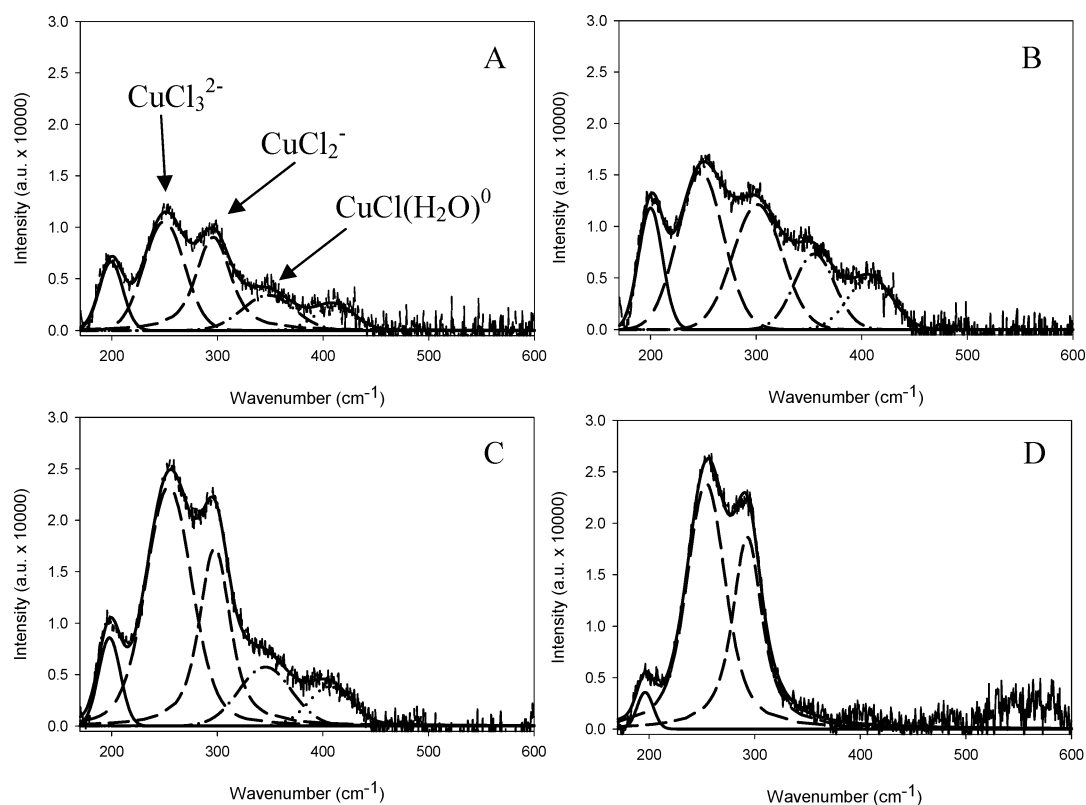


Figure 2. Raman spectra of copper(I) chloride in aqueous 6 mol·kg⁻¹ HCl solution at 25 °C: (A) 0.2494 mol·kg⁻¹, (B) 0.5968 mol·kg⁻¹, (C) 1.000 mol·kg⁻¹, and (D) 1.500 mol·kg⁻¹. Bands at 247 ± 3 and 297 ± 3 cm⁻¹ are assigned to $[\text{CuCl}_3]^{2-}$ and $[\text{CuCl}_2]^-$, respectively. The band at 350 ± 3 cm⁻¹ is assigned to $[\text{CuCl}(\text{H}_2\text{O})]^0$. The possible band ~ 410 cm⁻¹ is postulated to be a fragment of a higher frequency vibrational mode of $[\text{CuCl}(\text{H}_2\text{O})]^0$, which was obscured by the baseline subtraction procedure.

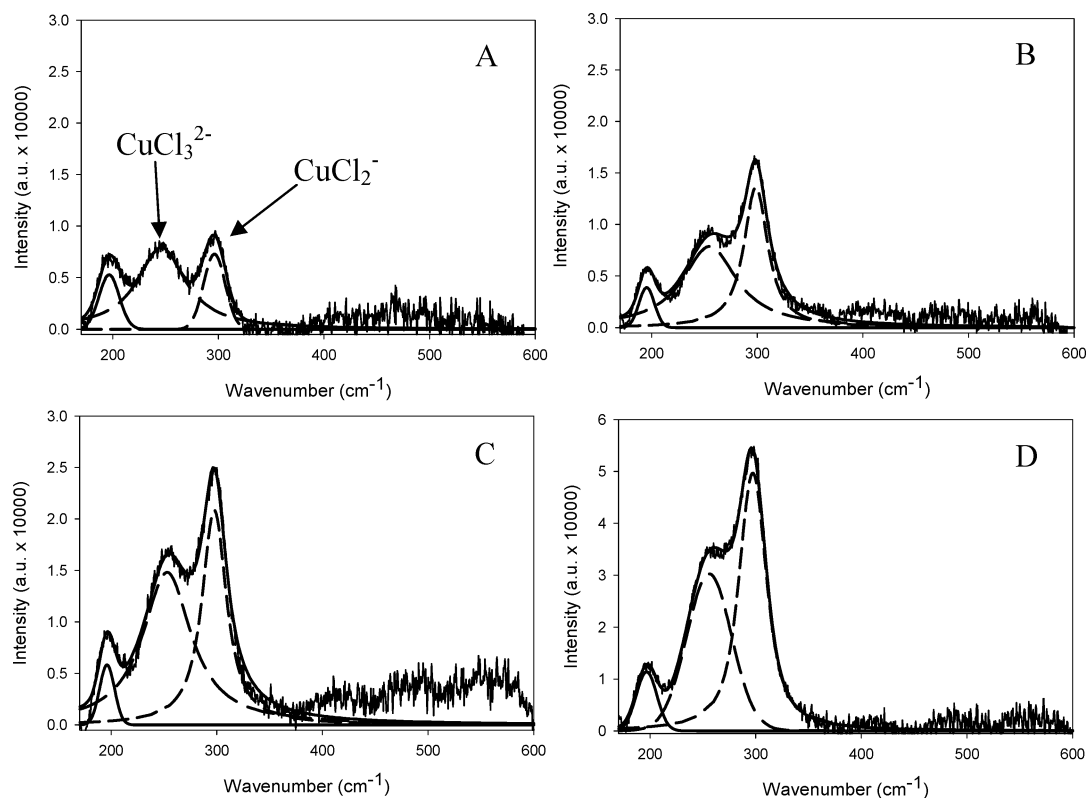


Figure 3. Raman spectra of copper(I) chloride in aqueous 6 mol·kg⁻¹ HCl solution at 80 °C: (A) 0.2494 mol·kg⁻¹, (B) 0.5968 mol·kg⁻¹, (C) 1.000 mol·kg⁻¹, and (D) 1.500 mol·kg⁻¹. Bands at 247 ± 3 and 297 ± 3 cm⁻¹ are assigned to $[\text{CuCl}_3]^{2-}$ and $[\text{CuCl}_2]^-$ respectively.

Table 2. Ab Initio Calculated and Experimental Frequencies of $[\text{Cu}(\text{H}_2\text{O})_2]^+$, $[\text{CuCl}(\text{H}_2\text{O})]^0$, $[\text{CuCl}_2]^-$, and $[\text{CuCl}_3]^{2-}$

aqueous species	symmetry	frequency (cm ⁻¹)				experimental
		calculated				
		basis set	HF	MP2	B3LYP	
Cu(H ₂ O) ₂ ⁺	D _{2d} /C ₂	6-31G*	362	493	488	~410?
		6-31+G*	278	396	372	
		6-311+G*	283	395	378	
Cu(H ₂ O) ₂ ⁺ (H ₂ O) ₄	D _{2d}	6-31G*	457	589 ^a	565 ^a	
		6-31+G*	373	505 ^a	467 ^a	
		6-311+G*	382	508	474	
CuCl(H ₂ O)	C _{2v/s}	6-31G*	331	414	394	~350
			436	541	510	~410?
		6-31+G*	260	362	327	
			379	487	438	
		6-311+G*	263	371	334	
CuCl(H ₂ O)(H ₂ O) ₆	C _s		379	490	446	
		6-31G*	312	429	392	
			498	638	611	
		6-31+G*	284	375	336	
			416	553	513	
CuCl ₂ ⁻	D _{∞h}	6-311+G*	280	365	334	
			422	559	514	
		6-31G*	262	337	308	297 ± 3
		6-31+G*	234	314	274	
		6-311+G*	232	305	271	
CuCl ₂ ⁻ (H ₂ O) ₆	S ₆ #1	6-31G*	273 ^a	354	330	
		6-31+G*	243 ^a	318	286	
		6-311+G*	240 ^a	314 ^a	284	
CuCl ₃ ²⁻	D _{3h}	6-31G*	162	202	202	247 ± 3
		6-31+G*	144	206	172	
		6-311+G*	146	199	175	
		6-31G*	188	227	220	
CuCl ₃ ²⁻ (H ₂ O) ₆	D _{3h}	6-31+G*	177	235	204	
			182	229 ^a	208	

^aThese structures possessed a small imaginary frequency.

The baseline-corrected reduced isotropic Raman spectra, $R_{\text{iso}}(\omega)$, for all the solutions at 25 and 80 °C are plotted in Figures 2 and 3, respectively. The vibrational bands for each species and their areas, were obtained from the baseline-corrected, reduced isotropic Raman spectra by fitting each band to the statistically significant set of Voigt functions using the curve fitting program, OriginPro version 8.5.1, and the default convergence criteria which corresponds to a standard error less than 5% of the baseline noise. The frequencies are tabulated in Table 2, along with the band assignments derived below.

The absence of copper(II) and colloidal copper from any redox or disproportionation reactions occurring up to 80 °C can be inferred because no color change to either the blue-green colored copper(II) complexes or the brown colloidal copper took place, and no precipitation was observed.

3.2. Ab Initio Results. Stable structures obtained from the ab initio calculations, corresponding to hydrated forms of the species $[\text{Cu}(\text{H}_2\text{O})_2]^+$, $[\text{CuCl}(\text{H}_2\text{O})]^0$, $[\text{CuCl}_2]^-$, and $[\text{CuCl}_3]^{2-}$, are shown in Figure 4. The predicted symmetric Raman bands of the model species are tabulated in Table 2, along with the experimental Raman peaks assigned to these bands in section 3.3. The aqua ion itself can potentially exist as a di-, tri-, or tetraordinated structure. For copper(I) with four water molecules, a plethora of structures exist in which the water molecules are either all bound to the copper (tetraordinate, [4+0]), where three are bound to the copper

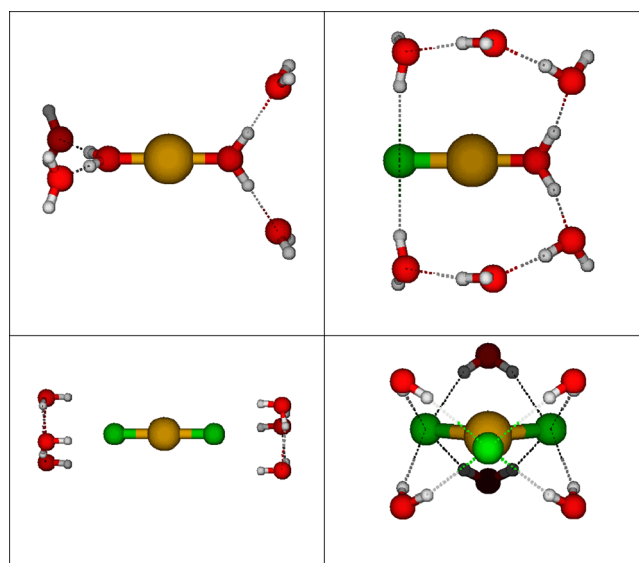


Figure 4. Selected ab initio structures of hydrated copper(I) chloride complexes, $\text{CuCl}_n(\text{H}_2\text{O})_m^{1-n}$, $n = 0-3$.

and one is in the second hydration shell (tricoordinate, [3+1]), or where two are bound to the copper and two are in the second hydration shell (dicoordinate, [2+2]). The existence of

Table 3. Calculated Equilibrium Concentrations of Copper(I) Chloride Species at 25 and 80 °C^a

temp (°C)	total $m(\text{Cu})$, mol·kg ⁻¹	$m([\text{CuCl}]^0)$, mol·kg ⁻¹	$m([\text{CuCl}_2]^-)$, mol·kg ⁻¹	$m([\text{CuCl}_3]^{2-})$, mol·kg ⁻¹	$m([\text{CuCl}_4]^{3-})$, mol·kg ⁻¹
25	0.2494	1.10×10^{-3}	1.33×10^{-1}	1.11×10^{-1}	4.24×10^{-3}
	0.5968	2.96×10^{-3}	3.38×10^{-1}	2.47×10^{-1}	7.73×10^{-3}
	1.0000	6.16×10^{-3}	6.02×10^{-1}	3.82×10^{-1}	1.05×10^{-2}
	1.5000	1.08×10^{-2}	9.69×10^{-1}	5.10×10^{-1}	1.06×10^{-2}
80	0.2494	1.13×10^{-3}	1.63×10^{-1}	8.34×10^{-2}	2.13×10^{-3}
	0.5968	2.95×10^{-3}	4.04×10^{-1}	1.86×10^{-1}	4.05×10^{-3}
	1.0000	5.96×10^{-3}	7.03×10^{-1}	2.85×10^{-1}	5.60×10^{-3}
	1.5000	1.01×10^{-2}	1.10×10^0	3.82×10^{-1}	5.94×10^{-3}

^aEquilibrium concentrations were calculated with MULTEQ chemical equilibrium software, using formation constants from Table 1. The species Cu^+ was omitted as all values were less than 5×10^{-7} mol·kg⁻¹.

these clusters, their symmetry, and their relative energy, depend greatly on the level. At the correlated levels, the [2+2] is more stable than the [3+1], which in turn is more stable than the [4+0], which suggests that copper(I) exists as the diaqua ion, shown in Figure 4, this structure is in agreement with other calculations by Feller et al.⁵¹ If diaquacopper(I) is present to any appreciable extent, then the band observed at around 410 cm⁻¹ in Figure 2 could be due to the Cu–O symmetric stretching motion. However, the calculations that include the second hydration sphere raise the vibrational frequency of the naked diaquacopper(I) cluster to around 500 cm⁻¹, which effectively rules this possibility out.

The neutral monochloro species is probably the main component of $\text{CuCl}(\text{g})$. In solution, however, the first water binds trans to the chloro ligand to form a [2+0] structure, shown in Figure 4. All of our attempts to find a minimum energy structure with three water molecules in the inner solvation shell resulted in the expulsion of a water ligand to give the [2+1] form. With three or more water molecules, some tetracoordinate species exist as minima at some levels, but these are not as stable as the tri- or dicoordinate species, which all possess hydrogen bonds. The diffuse function has a larger effect on the vibrational frequency, especially for the naked dicoordinate structure, than going from a double- ζ to triple- ζ valence basis set. For the hydrated species, the diffuse function is essential because without it, the hydrogens of the solvating water tend to interact directly with the copper atom instead of the chlorine atom. If the proposed assignment of the band at 350 cm⁻¹ to the O–Cu–Cl symmetric stretch is correct, then the Hartree–Fock theory clearly underestimates this frequency. The band resulting from the antisymmetric combination of Cu–Cl and Cu–O vibrations is calculated to be at much higher frequency than the possible band observed at ~410 cm⁻¹, for reasons discussed below.

As discussed below in section 3.2, the dichlorocuprate(I) ion is the major form of copper(I) in the presence of excess chloride ligand under the conditions used here. The ion is dicoordinate and linear. All attempts to add water molecules to the first solvation shell failed and resulted in expulsion of either water or chloride ligand. Numerous hydrated forms of the dichlorocuprate ion were also examined. For the calculated vibrational frequencies of naked dichlorocuprate(I), increasing the basis set size decreases the frequencies (Table 2). The diffuse function has a large effect on the calculated frequency, as would be expected for anions. However, going from a double- ζ to triple- ζ basis set has a small effect (except at the MP2 level). As the Hartree–Fock calculations already underestimate the vibrational frequency, improving the basis set worsens the agreement. The B3LYP/6-31G* and MP2/6-311+G* are in

reasonable agreement with experiment (within 10 cm⁻¹). Solvating the ion with six waters (arranged as water trimers capping the chloride ligands with nearly degenerate in energy S_6 , C_{3h} , or D_3 point group symmetry) increases the frequency by about 10 cm⁻¹.

The trichlorocuprate(II) ion is a minor form of copper(I) in the presence of excess chloride ligand. The ion is trigonal planar. Several hydrated forms of the trichlorocuprate ion were examined. For the calculated vibrational frequencies of naked trichlorocuprate(I), adding the diffuse function substantially decreases the calculated frequency (Table 2). Going from 6-31+G* to 6-311+G* increases slightly the frequency at the HF and B3LYP levels but decreases it at the MP2 level. Hydration has a much larger effect on this more highly charged ion, increasing the frequency by 20–35 cm⁻¹.

3.3. Interpretation of Raman Spectra and Band Assignment. Although the bands are very weak, the baseline-corrected reduced isotropic spectra in Figures 2 and 3 show evidence for five statistically significant Raman active peaks at 25 °C, and three at 80 °C, which can be resolved by the deconvolution method described above. The low frequency region below ~250 cm⁻¹ is characteristic of librational modes that reflect the structure and dynamics of water, and as a result, we conclude that the weak band at 200 ± 20 cm⁻¹ is due to hydration effects and that it can be excluded as a species.^{49,52–60} The two distinctive peaks at 297 ± 3 and 247 ± 3 cm⁻¹ occur in the frequency range identified by the ab initio calculations for copper species, described below.

The distribution of species in each of our experimental solutions, as calculated from the cumulative formation constants in Table 1, are listed in Table 3. The results show that our aqueous copper(I) chloride solutions contained two dominant species, $[\text{CuCl}_2]^-$ and $[\text{CuCl}_3]^{2-}$, with $[\text{CuCl}]^0$ present as a third minor species. The copper(I) aqua ion and tetrachlorocuprate(I) species in our solutions are not present at concentrations detectable by Raman spectroscopy. Hence we assign the bands at 297 ± 3 and 247 ± 3 cm⁻¹ to the two most intense copper–chloro Raman-active symmetric vibrational modes of the $[\text{CuCl}_2]^-$ and $[\text{CuCl}_3]^{2-}$ species. The chemical equilibrium calculations show that increasing the temperature shifts the equilibrium in favor of the less-highly charged species, $[\text{CuCl}_2]^-$. Comparing the equilibrium concentrations of these two species in Table 3, with the concentration and temperature dependence of the Raman bands in Figures 2 and 3 provides strong evidence that the band at 297 ± 3 cm⁻¹ arises from the species $[\text{CuCl}_2]^-$ and that the band at 247 ± 3 cm⁻¹ arises from $[\text{CuCl}_3]^{2-}$. These assignments are consistent with the results from ab initio calculations using density functional theory in Table 2, which predict that the peak position for the totally

Table 4. Normalized Peak Area of the Di- and Trichloro Copper Species at 25 and 80 °C

total $m(\text{Cu})$, (mol·kg ⁻¹)	normalized peak area ($A_{ij} \cdot m_{\text{IS}}/A_{\text{IS}}$)			
	25 °C		80 °C	
	$[\text{CuCl}_3]^{2-}$	$[\text{CuCl}_2]^-$	$[\text{CuCl}_3]^{2-}$	$[\text{CuCl}_2]^-$
0.2494	5.07×10^{-3}	4.78×10^{-3}	6.90×10^{-3}	1.87×10^{-3}
0.5968	8.30×10^{-3}	7.09×10^{-3}	7.72×10^{-3}	5.74×10^{-3}
1.0000	1.41×10^{-2}	8.20×10^{-3}	1.30×10^{-2}	8.95×10^{-3}
1.5000	1.35×10^{-2}	8.97×10^{-3}	1.62×10^{-2}	2.19×10^{-2}

Table 5. Reduced Raman Molar Scattering Coefficients $S_i/S_{\text{ClO}_4^-}$ ^a for the $[\text{CuCl}_3]^{2-}$ and $[\text{CuCl}_2]^-$ Species

temp (°C)	total $[\text{Cu}^+]$ (mol·kg ⁻¹)	$S_i/S_{\text{ClO}_4^-}$ for $[\text{CuCl}_3]^{2-}$	$S_i/S_{\text{ClO}_4^-}$ for $[\text{CuCl}_2]^-$
25	0.2494	(4.56×10^{-2})	(3.59×10^{-2})
	0.5968	3.35×10^{-2}	2.10×10^{-2}
	1.0000	3.69×10^{-2}	1.36×10^{-2}
	1.5000	2.65×10^{-2}	9.26×10^{-3}
80	0.2494	(8.27×10^{-2})	(1.15×10^{-2})
	0.5968	4.16×10^{-2}	1.42×10^{-2}
	1.0000	4.55×10^{-2}	1.27×10^{-2}
	1.5000	4.25×10^{-2}	1.99×10^{-2}
average ^b		$(3.77 \pm 0.64) \times 10^{-2}$	$(1.51 \pm 0.41) \times 10^{-2}$

^a $S_i/S_{\text{ClO}_4^-} = \left[\frac{A_{ij}}{A_{\text{IS}}} \cdot m_{\text{IS}} \right] \frac{1}{m_j}$ ^bValues obtained at 0.2494 mol kg⁻¹ have been omitted from the average due to large experimental uncertainties associated with low concentration and weak intensities.

symmetric Cu–Cl stretching bands of the species $[\text{CuCl}_2(\text{H}_2\text{O})_6]^-$ occurs at higher frequency than that of $[\text{CuCl}_3(\text{H}_2\text{O})_6]^{2-}$. The experimental values are most closely matched by the MP2 method using the 6-31+G* basis set, which predicts values of 318 cm⁻¹ for the species $[\text{CuCl}_2(\text{H}_2\text{O})_6]^-$ and 235 cm⁻¹ for $[\text{CuCl}_3(\text{H}_2\text{O})_6]^{2-}$.

The two bands at frequencies 350 ± 10 and 410 ± 20 cm⁻¹ in the dilute solutions at 25 °C, shown in Figure 2, may correspond to the monochlorocopper complex. The computational results in Table 2 for the species $[\text{CuCl}(\text{H}_2\text{O})]^\circ$ using the MP2 method with the 6-31+G* basis set show symmetric stretching bands at 362 and 487 cm⁻¹. The same calculations for the hydrated species $[\text{CuCl}(\text{H}_2\text{O})(\text{H}_2\text{O})_6]^\circ$ yield symmetric stretching frequencies at 375 and 553 cm⁻¹. The spectral resolution in the region above 400 cm⁻¹ is complicated by a weak perchlorate band at 464 cm⁻¹ and our baseline subtraction technique, which fixes the relative molar scattering coefficient to zero at 460 cm⁻¹. These effects were much more significant for spectrum D in Figure 2, in which these bands are very weak. The low intensity at this concentration is very probably an artifact of the baseline subtraction. These bands appear to be weak or absent in all the spectra at 80 °C. The quality of these spectra was equivalent to the best spectra at 25 °C, so their absence cannot be attributed to baseline subtraction artifacts. The concentration of $[\text{CuCl}]^\circ$ at 80 °C is lower than at 25 °C, relative to the other copper species, and it may be that these bands are below the limit of detection. We conclude that the band at 350 ± 10 cm⁻¹ is due to the symmetric O–Cu–Cl stretching mode of the hydrated monochloro species $[\text{CuCl}(\text{H}_2\text{O})]^\circ$ and that the band at 410 cm⁻¹ is a remnant of the low frequency wing of the predicted band at 553 cm⁻¹, heavily distorted by baseline subtraction. The 553 cm⁻¹ band is the antisymmetric stretching mode due to out-of-phase Cu–O and Cu–Cl motions. These bands were not well enough defined in our spectra to permit $[\text{CuCl}$

$(\text{H}_2\text{O})]^\circ$ to be included in the calculation of relative molar scattering coefficients described below.

3.4. Speciation Calculations. For the spectra of solutions containing multiple solutes, j , each with i vibrational bands, eqs 2–4 take the forms

$$I_{\text{iso}}(\omega) = C_{\text{Instr}}(\omega_0 - \omega)^4 \omega^{-1} B^{-1} \sum_j c_j \sum_i S_{ij}$$

$$= C_{\text{Instr}}(\omega_0 - \omega)^4 \omega^{-1} \sum_j c_j \sum_i J_{ij} \quad (5)$$

and

$$R_{\text{iso}}(\omega) = C_{\text{Instr}} \sum_j c_j \sum_i S_{ij} \quad (6)$$

where J_{ij} and S_{ij} are the isotropic Raman molar scattering coefficient and reduced Raman molar scattering coefficient,⁶¹ respectively. The reduced isotropic spectra $R_{\text{iso}}(\omega)$ are preferred for quantitative data treatments, rather than $I(\omega)$, because the integrated peak areas of the i vibrational bands, A_{ij} , for each species, j , are proportional to the molar concentration, c_j , at all temperatures and frequencies,

$$A_{ij} = S_{ij} c_j = S_{ij} m_j \rho_{\text{Soln}} \quad (7)$$

and because the removal of the $(\omega_0 - \omega)^4 \omega^{-1}$ term simplifies the baseline subtraction.^{40,41} The reduced molar scattering coefficient S_j is related to the isotropic molar scattering coefficient J_j by the relationship: $S_j = B J_j$.

For quantitative measurements, a noncomplexing anion such as perchlorate must be used as an internal reference standard. The integrated area of each band in the reduced isotropic spectra, relative to that of the $\nu_1(\text{ClO}_4^-)$ band at 936 cm⁻¹, yields the molality of the species relative to perchlorate:

$$A_{\text{IS}} = S_{\text{IS}} c_{\text{IS}} = S_{\text{IS}} m_{\text{IS}} \rho_{\text{Soln}} \quad (8)$$

and, if the reduced molar scattering coefficient relative to perchlorate, S_i/S_{IS} , is known:

$$m_i = \left(\frac{A_i}{A_{\text{IS}}} \right) \left(\frac{S_{\text{IS}}}{S_i} \right) m_{\text{IS}} \quad (9)$$

The changes in the intensity of the Raman bands with temperature and concentration, which result from changes in the equilibrium between the species, provide a strong tool for assigning the bands to individual $[\text{CuCl}_n]^{1-n}$ species. The relative abundances of the species in our solutions were calculated at 25 and 80 °C from refitted values of the formation constants reported by Liu et al.,²⁸ which are listed in Table 2 for a wide range of temperatures, using the chemical modeling software MULTEQ. The results are tabulated in Table 3.

A particularly rigorous test is to calculate the Raman molar scattering coefficients of these species (S_{ij}), using the copper chloride formation constants reported by Liu et al.,²⁸ and to determine whether they are independent of temperature and concentration, as predicted by eqs 8 and 9. Values for the integrated peak area of the vibrational band for each species, normalized to the perchlorate band, $(A_{ij}/A_{\text{ClO}_4^-}) \cdot m_{\text{ClO}_4^-}$, are listed in Table 4. The reduced Raman molar scattering coefficients relative to perchlorate, $S_i/S_{\text{ClO}_4^-}$, are tabulated in Table 5 and plotted as a function of molality in Figures 5 and 6,

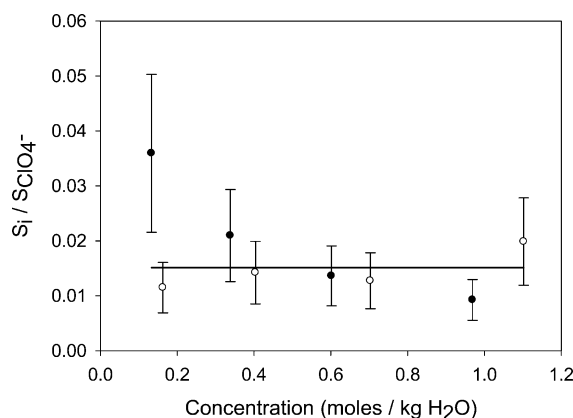


Figure 5. Experimental reduced Raman molar scattering coefficients, $S_i/S_{\text{ClO}_4^-}$, for $[\text{CuCl}_2]^-$ (aq) at 25 °C (●) and 80 °C (○). The values for 0.25 mol·kg⁻¹ have been omitted from the average, which is shown by the horizontal line.

along with their uncertainty limits. The reduced molar scattering coefficients for both species are independent of temperature and concentration to within the combined experimental uncertainties, yielding the values $S_{\text{CuCl}_2^-}/S_{\text{ClO}_4^-} = (1.51 \pm 0.41) \times 10^{-2}$ and $S_{\text{CuCl}_3^{2-}}/S_{\text{ClO}_4^-} = (3.77 \pm 0.64) \times 10^{-2}$. This is strong evidence that the band assignments and thermodynamic model used in the calculations are correct. We note that our use of the formation constants reported by Liu et al.²⁸ is not compromised by more recent XAS observations that $[\text{CuCl}_4]^{3-}$ is not stable,^{13,35} because the calculated concentrations in our measurements, listed in Table 3, are less than 1%.

Gas-phase measurements strongly suggest that copper(I) exists mainly as the diaqua ion, $[\text{Cu}(\text{H}_2\text{O})_2]^+$, because of the large difference between the second and third incremental hydration enthalpies.^{62,63} In addition to demonstrating this

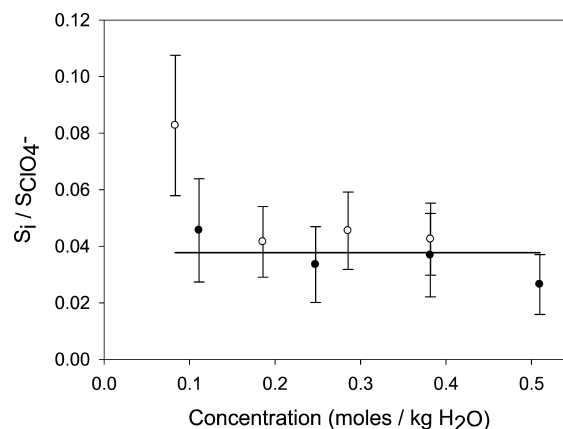


Figure 6. Experimental reduced Raman molar scattering coefficient, $S_i/S_{\text{ClO}_4^-}$, for $[\text{CuCl}_3]^{2-}$ at 25 °C (●) and 80 °C (○). The values for 0.25 mol·kg⁻¹ have been omitted from the average, which is shown by the horizontal line.

preference, our calculations also show a strong preference for the dicoordinate chloroaquacopper(I) and the di- and trichlorocuprate(I) ions. The calculated frequencies, at the highest level examined (MP2/6-311+G*) are in good agreement with the assigned frequencies. It has been shown (Table 2) that to match experiment reasonably well, it is important to use a basis set that includes diffuse functions. There is not a big difference between frequencies calculated with the double- ζ valence 6-31+G* and triple- ζ valence 6-311+G* basis sets. Hartree–Fock calculations will underestimate the vibrational frequencies, especially as the negative charge on the anions increases.

4. DISCUSSION

For the reasons presented above, there is strong evidence for assigning the bands at 297 ± 3 and 247 ± 3 cm⁻¹ to the ν_1 symmetric stretching vibrations of the aqueous $[\text{CuCl}_2]^-$ and $[\text{CuCl}_3]^{2-}$ species. In addition, there is reasonable evidence that the band at 350 ± 10 cm⁻¹ is due to the symmetric Cu–Cl stretching mode of the hydrated monochloro species $[\text{CuCl}(\text{H}_2\text{O})]^0$. We are aware of only one previous Raman study on Cu(I) chloride solutions with which to compare these results, a solvent extraction study by Creighton and Lippincott²⁴ with spectra for 1.6 M solution of H_2CuCl_3 in equilibrium with an aqueous solution of 3 M CuCl in 8.4 M HCl. The spectra of the ether solution showed a symmetric band at 296 cm⁻¹, which was assigned to the linear complex $[\text{CuCl}_2]^-$, identical to our experimental result for the same species in aqueous solution. The fact that the same result is obtained in water and ethyl ether indicates that the solvation effects are weak, consistent with the structure in Figure 4. The aqueous phase showed a diffuse band at ~ 220 cm⁻¹, which could not be resolved, consistent with the accurate spectra shown in Figures 2 and 3, from our more modern instrument.

Recently, Sherman³⁵ and Brugger et al.³⁶ have reported ab initio molecular dynamics simulations of the Cu(I) chloride solutions at concentrations up to 4 mol kg⁻¹, and temperatures up to 450 °C. These treatments used the Car–Parrinello method to solve the classical equations of motion while treating the interatomic interactions quantum mechanically. Sherman's³⁵ study showed that Cu(I) exists as $[\text{CuCl}_3]^{2-}$ in a 4 mol kg⁻¹ solution at room temperature. This is a distorted linear $[\text{CuCl}_2]^-$ complex with weak ion-pairing to a third

chloride. A linear $[\text{CuCl}_2]^-$ complex predominates under hydrothermal conditions. The tetrahedral $[\text{CuCl}_4]^{3-}$ complex proposed by Liu et al.²⁸ from UV–visible measurements was found to be unstable. Independent studies using X-ray absorption methods by Brugger et al.¹³ and Fulton et al.¹⁷ confirmed these findings. They observed linear complexes of $[\text{CuCl}(\text{H}_2\text{O})]^0$ and $[\text{CuCl}_2]^-$ at elevated temperatures, with low concentrations of $[\text{CuCl}_3]^{2-}$ as a trigonal planar complex at low temperatures. These are consistent with the structures for the hydrated species from our ab initio calculations shown in Figure 4.

5. CONCLUSION

The Raman spectra of copper(I) chloride solutions have been measured up to temperatures up to 80 °C. Preparing stable concentrated solutions of Cu(I) chloride was very challenging, because the solubility limit of copper(I) chloride at room temperature (20 °C) in 6 mol L⁻¹ HCl is only 1.66 mol L⁻¹,^{11,64} and because copper(I) disproportionated into Cu(II) and Cu(s) above 100 °C. Although the intensity of the copper–chloro bands is very weak, a stable Raman signal and rigorous baseline subtraction techniques allowed us to obtain quantitative spectra. To our knowledge, these are the first accurate Raman spectra reported for aqueous copper(I) chloro complexes. The spectra are consistent with hydrated mono-nuclear monochloro, dichloro and trichloro complexes, $[\text{CuCl}(\text{H}_2\text{O})]^0$, $[\text{CuCl}_2]^-$, and $[\text{CuCl}_3]^{2-}$, and with the temperature dependent formation constants reported by Liu et al.²⁸

Our study also showed that, to achieve reasonable agreement with experiment for Cu(I) chloro-complexes, ab initio calculations must include the effect of the solvent. The challenge in treating waters of solvation for these complexes is that the ion–ion and ion–water interactions are weak, so that the selection of basis sets must be done with care and enough waters must be included to approximate the fully solvated ion. This is reflected in Pearson's classical nomenclature, which describes Cu^+ as a “soft” Lewis acid while H_2O and Cl^- are “hard” Lewis bases. Ab initio calculations, when done at a sufficiently high level and with the appropriate number of hydrating water molecules, support the proposed assignments.

One of the objectives of this work was to determine whether Raman spectroscopy can be used as a practical tool to obtain quantitative equilibrium constants and structural information for transition metal complexes in high-pressure cells under hydrothermal conditions. Although the copper(I) chloride study was limited to low temperatures because of its sensitivity to redox effects and disproportionation at temperatures above 100 °C, the results reported here do show that such measurements can be made successfully. The principal challenge arises from the very weak Raman scattering coefficients, which are probably typical of most first-row transition metal chlorides, hydroxides and hydrogen sulfides. Successful application of the method to other metal–ligand systems will require concentrations above 1 mol kg⁻¹, relatively simple speciation, and no complications from colored solutions or fluorescence effects.

AUTHOR INFORMATION

Notes

The authors declare no competing financial interest.

[§]C. C. Pye: e-mail, cory.pye@smu.ca.

^{||}P. R. Tremaine, e-mail: tremaine@uoguelph.ca.

ACKNOWLEDGMENTS

Financial support of the Natural Science and Engineering Council of Canada (NSERC), the Ontario Research Foundation and the NSERC/NRCan/AECL Joint Research Program on Supercritical-Water-Reactor Chemistry is gratefully acknowledged. C.R.C. and D.J.W.M. acknowledge the support of the Nova Scotia Department of Economic Development for co-operative education salary support (C.R.C., Work Term 2, Jan–Apr 2001; D.J.W.M., Work Term 2, Sep–Dec 2002). We thank Daniel C. M. Whynot for critically examining the preliminary ab initio calculations. Dr. Jenny Cox, Dr. Yohann Coulier and one of the Reviewers for this journal provided valuable and insightful comments on the manuscript.

REFERENCES

- (1) Guzonas, D. A.; Cook, W. G. Cycle Chemistry and its Effect on Materials in a Supercritical Water-Cooled Reactor: A Synthesis of Current Understanding. *Corros. Sci.* **2012**, *65*, 48–66.
- (2) Naterer, G. F.; et al. Canada's Program on Nuclear Hydrogen Production and the Thermochemical Cu–Cl Cycle. *Int. J. Hydrogen Energy* **2010**, *35*, 10905–10926.
- (3) Zajacz, Z.; Seo, J. H.; Candela, P. A.; Piccoli, P. M.; Tossell, J. A. The Solubility of Copper in High-Temperature Magmatic Vapors: A Quest for the Significance of various Chloride and Sulfide Complexes. *Geochim. Cosmochim. Acta* **2011**, *75*, 2811–2827.
- (4) Sillitoe, R. H. Porphyry Copper Systems. *Econ. Geol.* **2010**, *105*, 3–41.
- (5) Crerar, D. A.; Barnes, H. L. Ore Solution Chemistry V. Solubilities of Chalcopyrite and Chalcocite Assemblages in Hydrothermal Solutions at 200 and 300 °C. *Econ. Geol.* **1976**, *71*, 772–794.
- (6) Ahrland, S.; Rawsthorne, J. The Stability of Metal Halide Complexes in Aqueous Solution. VII. the Chloride Complexes of Copper(I). *Acta Chem. Scand.* **1970**, *24*, 157–172.
- (7) Mountain, B. W.; Seward, T. M. The Hydrosulphide Complexes of Copper(I): Experimental Determination of Stoichiometry and Stability at 22 °C and Reassessment of High Temperature Data. *Geochim. Cosmochim. Acta* **1999**, *63*, 11–29.
- (8) Mountain, B. W.; Seward, T. M. Hydrosulphide/Sulphide Complexes of Copper(I): Experimental Confirmation of the Stoichiometry and Stability of $\text{Cu}(\text{HS})_2^-$ to Elevated Temperatures. *Geochim. Cosmochim. Acta* **2003**, *63*, 11–29.
- (9) Sharma, V. K.; Millero, F. J. Equilibrium Constants for the Formation of Cu(I) Halide Complexes. *J. Solution Chem.* **1990**, *19*, 375–390.
- (10) Fritz, J. J. Chloride Complexes of CuCl in Aqueous Solutions. *J. Phys. Chem.* **1980**, *84*, 2241–2246.
- (11) Fritz, J. J. Solubility of Cuprous Chloride in various Soluble Aqueous Chlorides. *J. Chem. Eng. Data* **1982**, *27*, 188–193.
- (12) Brugger, J.; McPhail, D. C.; Black, J.; Spiccia, L. Complexation of Metal Ions in Brines: Application of Electronic Spectroscopy in the Study of the Cu(II)–LiCl–H₂O System between 25 and 90 °C. *Geochim. Cosmochim. Acta* **2001**, *65*, 2691–2708.
- (13) Brugger, J.; Etschmann, B.; Liu, W.; Testemale, D.; Hazemann, J. L.; Emerich, H.; van Beek, W.; Proux, O. An XAS Study of the Structure and Thermodynamics of Cu(I) Chloride Complexes in Brines Up to High Temperature (400 °C, 600 bar). *Geochim. Cosmochim. Acta* **2007**, *71*, 4920–4941.
- (14) Trevani, L.; Ehlerova, J.; Sedlbauer, J.; Tremaine, P. R. Complexation in the Cu(II)–LiCl–H₂O System at Temperatures to 423 K by UV-Visible Spectroscopy. *Int. J. Hydrogen Energy* **2010**, *35*, 4893–4900.
- (15) Lundstrom, M.; Aromaa, J.; Forsen, O.; Hyvarinen, I.; Barker, M. H. Leaching of Chalcopyrite in Cupric Chloride Solution. *Hydrometallurgy* **2005**, *77*, 89–95.
- (16) D'Angelo, P.; Bottari, E.; Festa, M. R.; Nolting, H.; Pavel, N. V. Structural Investigation of Copper(II) Chloride Solutions using X-Ray Absorption Spectroscopy. *J. Chem. Phys.* **1997**, *107*, 2807–2812.

- (17) Fulton, J. L.; Hoffmann, M. M.; Darab, J. G.; Palmer, B. J.; Stern, E. A. Copper(I) and Copper(II) Coordination Structure Under Hydrothermal Conditions at 325 °C: An X-Ray Absorption Fine Structure and Molecular Dynamics Study. *J. Phys. Chem. A* **2000**, *104*, 11651–11663.
- (18) Li, G.; Camaioni, D. M.; Amonette, J. E.; Zhang, C. Z.; Johnson, T. J.; Fulton, J. L. $[\text{CuCl}_n]^{2-n}$ Ion-Pair Species in 1-Ethyl-3-Methylimidazolium Chloride Ionic Liquid-Water Mixtures: Ultra-violet-Visible, X-Ray Absorption Fine Structure, and Density Functional Theory Characterization. *J. Phys. Chem. B* **2010**, *114*, 12614–12622.
- (19) Yi, H. B.; Xia, F. F.; Zhou, Q.; Zeng, D. CuCl_3^- and CuCl_4^{2-} Hydrates in Concentrated Aqueous Solution: A Density Functional Theory and ab initio Study. *J. Phys. Chem. A* **2011**, *115*, 4416–4426.
- (20) Xia, F.; Yi, H.; Zeng, D. Hydrates of Cu^{2+} and CuCl^+ in Dilute Aqueous Solution: A Density Functional Theory and Polarized Continuum Model Investigation. *J. Phys. Chem. A* **2010**, *114*.
- (21) Sherman, D. M. Metal Complexation and Ion Association in Hydrothermal Fluids: Insights from Quantum Chemistry and Molecular Dynamics. *Geofluids* **2010**, *10*, 41–57.
- (22) Voigt, W.; Zhou, Q.; Zeng, D. Thermodynamic Modeling of Salt-Water Systems Up to Saturation Concentrations Based on Solute Speciation: $\text{CuCl}_2\text{-MCl}_n\text{-H}_2\text{O}$ at 298 K ($M = \text{Li, Mg, Ca}$). *Fluid Phase Equilib.* **2012**, *322–323*, 30–40.
- (23) Sugasaka, K.; Fujii, A. Spectroscopic Study of Copper(I) Chloro Complexes in Aqueous 5M $\text{Na}(\text{Cl, ClO}_4)$ Solutions. *Bull. Chem. Soc. Jpn.* **1976**, *49*, 82–86.
- (24) Creighton, J. A.; Lippincott, E. R. Raman Spectra and Solvent-Extractions of Cuprous Halides. *J. Chem. Soc.* **1963**, Nov., 5134–5136.
- (25) Xiao, Z. F.; Gammons, C. H.; Williams-Jones, A. E. Experimental Study of Copper(I) Chloride Complexing in Hydrothermal Solutions at 40 to 300 °C and Saturated Water Vapor Pressure. *Geochim. Cosmochim. Acta* **1998**, *62*, 2949–2964.
- (26) Hack, A. C.; Mavrogenes, J. A. A Synthetic Fluid Inclusion Study of Copper Solubility in Hydrothermal Brines from 525 to 725 °C and 0.3 to 1.7 GPa. *Geochim. Cosmochim. Acta* **2006**, *70*, 3970–3985.
- (27) Liu, W. H.; McPhail, D. C.; Brugger, J. An Experimental Study of Copper(I)-Chloride and Copper(I)-Acetate Complexing in Hydrothermal Solutions between 50 and 250 °C and Vapor-Saturated Pressure. *Geochim. Cosmochim. Acta* **2001**, *65*, 2937–2948.
- (28) Liu, W. H.; Brugger, J.; McPhail, D. C.; Spiccia, L. A Spectrophotometric Study of Aqueous Copper(I)-Chloride Complexes in LiCl Solutions between 100 and 250 °C. *Geochim. Cosmochim. Acta* **2002**, *66*, 3615–3633.
- (29) Fulton, J. L.; Hoffmann, M. M.; Darab, J. G. An X-Ray Absorption Fine Structure Study of Copper(I) Chloride Coordination Structure in Water Up to 325 °C. *Chem. Phys. Lett.* **2000**, *330*, 300–308.
- (30) Mavrogenes, J. A.; Berry, A. J.; Newville, M.; Sutton, S. R. Copper Speciation in Vapor-Phase Fluid Inclusions from the Mole Granite, Australia. *Am. Mineral.* **2002**, *87*, 1360–1364.
- (31) Berry, A. J.; Hack, A. C.; Mavrogenes, J. A.; Newville, M.; Sutton, S. R. A XANES Study of Cu Speciation in High-Temperature Brines using Synthetic Fluid Inclusions. *Am. Mineral.* **2006**, *91*, 1773–1782.
- (32) Berry, A. J.; Harris, A. C.; Kamenetsky, V. S.; Newville, M.; Sutton, S. R. The Speciation of Copper in Natural Fluid Inclusions at Temperatures Up to 700 °C. *Chem. Geol.* **2009**, *259*, 2–7.
- (33) Liu, W.; Brugger, J.; Etschmann, B.; Testemale, D.; Hazemann, J. The Solubility of Nantokite ($\text{CuCl}(\text{s})$) and Cu Speciation in Low-Density Fluids Near the Critical Isochore: An in-Situ XAS Study. *Geochim. Cosmochim. Acta* **2008**, *72*, 4094–4106.
- (34) Etschmann, B. E.; Black, J. R.; Grundler, P. V.; Borg, S.; Brewe, D.; McPhail, D. C.; Spiccia, L.; Brugger, J. Copper(I) Speciation in Mixed Thiosulfate-Chloride and Ammonia-Chloride Solutions: XAS and UV-Visible Spectroscopic Studies. *RSC Adv.* **2011**, *1*, 1554–1566.
- (35) Sherman, D. M. Complexation of Cu^+ in Hydrothermal NaCl Brines: ab initio Molecular Dynamics and Energetics. *Geochim. Cosmochim. Acta* **2007**, *71*, 714–722.
- (36) Brugger, J.; Mei, Y.; Sherman, D. M.; Liu, W. ab initio Molecular Dynamics Simulation and Free Energy Exploration of Copper(I) Complexation by Chloride and Bisulfide in Hydrothermal Fluids. *Geochim. Cosmochim. Acta* **2013**, *102*, 45–64.
- (37) Hikita, H.; Ishikawa, H.; Esaka, N. Solubility and Equilibrium of Copper(I) Chloride in Hydrochloric-Acid Solutions. *Nippon Kagaku Kaishi* **1973**, *1*, 13–18.
- (38) Ciavatta, L.; Iuliano, M. Copper(I) Chloride Complexes in Aqueous Solution. *Ann. Chim.-Rome* **1998**, *88*, 71–89.
- (39) McConnell, H.; Davidson, N. Optical Interaction between the Chloro-Complexes of Copper(I) and Copper(II) in Solutions of Unit Ionic Strength. *J. Am. Chem. Soc.* **1950**, *72*, 3168–3173.
- (40) Rudolph, W. Structure and Dissociation of the Hydrogen Sulphate Ion in Aqueous Solution Over a Broad Temperature Range: A Raman Study. *Z. Phys. Chem* **1996**, *194*, 73–95.
- (41) Rudolph, W. W.; Pye, C. C. Raman Spectroscopic Measurements of Scandium(III) Hydration in Aqueous Perchlorate Solution and ab initio Molecular Orbital Studies of Scandium(III) Water Clusters: Does $\text{Sc}(\text{III})$ Occur as a Hexaqua Complex? *J. Phys. Chem. A* **2000**, *104*, 1627–1639.
- (42) Rudolph, W. W.; Fischer, D.; Irmer, G.; Pye, C. C. Hydration of Beryllium(II) in Aqueous Solutions of Common Inorganic Salts. A Combined Vibrational Spectroscopic and ab initio Molecular Orbital Study. *Dalton Trans.* **2009**, 6513–6527.
- (43) Rudolph, W. W. Raman and Infrared Spectroscopic Investigation of Speciation in $\text{BeSO}_4(\text{aq})$. *J. Solution Chem.* **2010**, *39*, 1039–1059.
- (44) Pye, C. C. An ab Initio Investigation of Lithium Ion Hydration. II. Tetra- Versus Hexacoordination and Halide Complexes. *Int. J. Quantum Chem.* **2000**, *76*, 62–76.
- (45) Pye, C. C.; Corbeil, C. R.; Rudolph, W. W. An ab Initio Investigation of Zinc Chloro Complexes. *Phys. Chem. Chem. Phys.* **2006**, *8*, 5428–5436.
- (46) Pye, C. C.; Corbeil, C. R. An ab Initio Investigation of Scandium Chloro Complexes. *Can. J. Chem.* **2002**, *80*, 1331–1342.
- (47) Lindsay, W. T. In *Chemistry Steam Cycle Solutions*; Cohen, P., Ed.; The ASME Handbook on Water Technology for Thermal Power Systems; American Society Mechanical Engineers: New York, 1990; pp 341–544.
- (48) Frisch, M. J.; Trucks, G. W.; Schlegel, H. B.; Scuseria, G. E.; Robb, M. A.; Cheeseman, J. R.; Zakrzewski, V. G.; Montgomery, J. A., Jr.; Stratmann, R. E.; Burant, J. C.; Dapprich, S.; Millam, J. M.; Daniels, A. D.; Kudin, K. N.; Strain, M. C.; Farkas, O.; Tomasi, J.; Barone, V.; Cossi, M.; Cammi, R.; Mennucci, B.; Pomelli, C.; Adamo, C.; Clifford, S.; Ochterski, J.; Petersson, G. A.; Ayala, P. Y.; Cui, Q.; Morokuma, K.; Malick, D. K.; Rabuck, A. D.; Raghavachari, K.; Foresman, J. B.; Cioslowski, J.; Ortiz, J. V.; Baboul, A. G.; Stefanov, B. B.; Liu, G.; Liashenko, A.; Piskorz, P.; Komaromi, I.; Gomperts, R.; Martin, R. L.; Fox, D. J.; Keith, T.; M. A. Al-Laham, Peng, C. Y.; Nanayakkara, A.; Challacombe, M.; Gill, P. M. W.; Johnson, B.; Chen, W.; Wong, M. W.; Andres, J. L.; Gonzalez, C.; M. Head-Gordon, Replogle, E. S.; Pople, J. A. *Gaussian 98*, Revision A.9; Gaussian, Inc., Pittsburgh PA, 1998.
- (49) Brooker, M. H.; Nielson, O. F.; Praestgaard, E. Assessment of Correction Procedures for Reduction of Raman-Spectra. *J. Raman Spectrosc.* **1988**, *19*, 71–78.
- (50) Rudolph, W. W. Raman-Spectroscopic Measurements of the First Dissociation Constant of Aqueous Phosphoric Acid Solution from 5 to 301 °C. *J. Solution Chem.* **2012**, *41*, 630–645.
- (51) Feller, D.; Glendening, E. D.; de Jong, W. A. Structures and Binding Enthalpies of $\text{M}^+(\text{H}_2\text{O})_n$ Clusters, $M = \text{Cu, Ag, Au}$. *J. Chem. Phys.* **1999**, *110*, 1475–1491.
- (52) Cabannes, J.; Rocard, Y. The Electromagnetic Theory of Maxwell-Lorentz and the Molecular Diffusion of Light. *J. Phys.-Paris* **1929**, *10*, 52–71.

- (53) Bucaro, J. A.; Litovitz, T. A. Molecular Motions in CCl_4 - Light Scattering and Infrared Absorption. *J. Chem. Phys.* **1971**, *55*, 3585–3588.
- (54) Bucaro, J. A.; Litovitz, T. A. Rayleigh Scattering - Collisional Motions in Liquids. *J. Chem. Phys.* **1971**, *54*, 3846–3853.
- (55) Nielsen, O. F.; Lund, P. A. Low-Frequency Raman-Spectra of Liquid Formamides and Aqueous-Solutions of Formamide. *Chem. Phys. Lett.* **1981**, *78*, 626–628.
- (56) Nielsen, O. F.; Lund, P. A.; Praestgaard, E. Comments on the $R(V)$ Spectral Representation of the Low-Frequency Raman-Spectrum. *J. Chem. Phys.* **1981**, *75*, 1586–1587.
- (57) Nielsen, O. F.; Lund, P. A.; Praestgaard, E. Low-Frequency Vibrations ($20\text{--}400\text{ cm}^{-1}$) of some Mono-Nucleotides in Aqueous-Solutions. *J. Raman Spectrosc.* **1981**, *11*, 92–95.
- (58) Perrot, M.; Brooker, M. H.; Lascombe, J. Raman Light-Scattering-Studies of the Depolarized Rayleigh Wing of Liquids and Solutions. *J. Chem. Phys.* **1981**, *74*, 2787–2794.
- (59) Lund, P. A.; Nielsen, O. F.; Praestgaard, E. Comparison of Depolarized Rayleigh-Wing Scattering and Far-Infrared Absorption in Molecular Liquids. *Chem. Phys.* **1978**, *28*, 167–173.
- (60) Murphy, W. F.; Brooker, M. H.; Nielsen, O. F.; Praestgaard, E.; Bertie, J. E. Further Assessment of Reduction Procedures for Raman-Spectra. *J. Raman Spectrosc.* **1989**, *20*, 695–699.
- (61) Schrader, B.; Moore, D. S. Nomenclature, Symbols, Units, and their Usage in Spectrochemical Analysis. XVIII. Laser-Based Molecular Spectroscopy for Chemical Analysis - Raman Scattering Processes. *Pure Appl. Chem.* **1997**, *69*, 1451–1468.
- (62) Magnera, T. F.; David, D. E.; Stulik, D.; Orth, R. G.; Jonkman, H. T.; Michl, J. Production of Hydrated Metal-Ions by Fast Ion Or Atom Beam Sputtering - Collision-Induced Dissociation and Successive Hydration Energies of Gaseous Cu^+ with 1–4 Water-Molecules. *J. Am. Chem. Soc.* **1989**, *111*, 5036–5043.
- (63) Dalleska, N. F.; Honma, K.; Sunderlin, L. S.; Armentrout, P. B. Solvation of Transition-Metal Ions by Water. Sequential Binding-Energies of $\text{M}^+(\text{H}_2\text{O})_x$ ($x = 1\text{--}4$) for $\text{M} = \text{Ti}$ to Cu Determined by Collision-Induced Dissociation. *J. Am. Chem. Soc.* **1994**, *116*, 3519–3528.
- (64) Fritz, J. J.; Koenigsberger, E.; Petrenko, S. V. In *Solubility data. Copper(I) Chloride-Water System*; Fritz, J. J., Koenigsberger, E., Eds.; Copper(I) Halides and Pseudohalides; Oxford University Press: Oxford, U.K., 1996; Vol. 65, pp 1–291.